

## Supporting Information

# “Mechanochemical synthesis of mechanical bonds in $M_{12}L_8$ poly- $[n]$ -catenanes.”

Javier Martí-Rujas<sup>a,b</sup>, Stefano Elli<sup>a</sup>, Alessandro Sacchetti<sup>a</sup>, and Franca Castiglione<sup>a</sup>

<sup>a</sup> Dipartimento di Chimica Materiali e Ingegneria Chimica “Giulio Natta”,  
Politecnico di Milano, Via L. Mancinelli 7, 20131 Milan, Italy.

<sup>b</sup> Center for Nano Science and Technology@Polimi, Istituto Italiano di  
Tecnologia, Via Pascoli 70/3, 20133 Milano, Italy.

# Contents

- **Materials and methods**
- **Single Crystal X-ray Diffraction**
- **Powder X-Ray Diffraction Experiments**
- **ATR-FT-IR Experiments**
- **Elemental Analysis Experiments**
- **TG experiments**
- **High-resolution solid-state NMR spectroscopy**
- **References**

## **Materials and Methods.**

### **Single Crystal X-ray Diffraction**

Single crystal X-ray data of poly-[*n*]-catenane **1** was measured using a Bruker D8 VENTURE diffractometer. The X-ray intensity data were measured using  $\lambda = 1.54178 \text{ \AA}$ .

### **Powder X-Ray Diffraction Experiments**

All the powder X-ray diffraction experiments were carried out using a Bruker D2-Phaser diffractometer equipped with Cu radiation ( $\lambda = 1.54184 \text{ \AA}$ ) using Bragg-Brentano geometry.

The experiments were performed at room temperature.

### **ATR-FT-IR Experiments**

ATR-FT-IR experiments were carried out on a FT-IR spectrometer: Varian 640-IR FT-IR spectrometer, A.T.R. equipped.

### **Elemental Analysis Experiments**

The elemental analysis experiments were carried out using a Costech ECS mod. 4010 at the Laboratorio Analisi Chimiche at Politecnico di Milano.

### **TG experiments**

Thermogravimetric analysis was carried out using a Perkin Elmer Thermal Analysis instrument at the Laboratorio Analisi Chimiche at the Dipartimento di Chimica, Materiali ed Ingegneria Chimica, Politecnico di Milano. The analyzed microcrystalline samples were heated within the temperature range from 30 °C to 700 °C using a heating rate of 10 °C/min under N<sub>2</sub>.

### **High-resolution solid-state NMR spectroscopy**

The solid-state MAS NMR experiments were carried out on a BRUKER NEO spectrometer equipped with a commercial 4 mm MAS iProbe. The magnetic field strength was 11.74 T corresponding to a  $^{13}\text{C}$  NMR resonance frequency of 125.75 MHz. Samples were packed into 4 mm  $\text{ZrO}_2$  rotor and spun at the magic angle with a spinning speed of 12 kHz for all the experiments. High-power proton decoupling (HPDEC) MAS NMR spectra were recorded after an excitation with a  $\pi/2$  pulse of 3.8  $\mu\text{s}$ , with a repetition time of 10 s and 3000 scans. Cross-polarization CPMAS NMR spectra were performed with a contact time of 2 ms, a repetition time of 4 s and 6500 scans, respectively. In the CPNQS experiments, the magnetization of the non-quaternary carbons (i.e., in solid-state  $^{13}\text{C}$  NMR the carbon not attached to any protons is called 'quaternary' even though this is inaccurate for unsaturated carbons such as in our case where it is only attached to only three other carbons) was dephased during a 60  $\mu\text{s}$  preacquisition delay with no proton decoupling. A total of 3600–4800 scans were required to obtain spectra with adequate signal-to-noise ratio. All the experiments have been performed at 298 K.  $^{13}\text{C}$  HPDEC MAS spectra of the crystalline poly- $[n]$ -catenane **1** have been acquired also in the temperature range 278–318 K.

## Mechanochemical synthesis of amorphous poly-[*n*]-catenane (**a1**) using LAG.

Ligand **TPB** (30 mg/0.097 mmol) was mixed with  $\text{ZnBr}_2$  (0.1455 mmol) and one drop of MeOH was added before grinding started. A total 61.3 mg were collected. The sample was used to measure TG which showed that some solvent was trapped in the material. Considering the hygroscopic nature of  $\text{ZnBr}_2$  and the low boiling point of methanol, we have considered that most likely the trapped guest is water. We decided not to treat in the oven the amorphous phase to avoid any alteration on the structure.

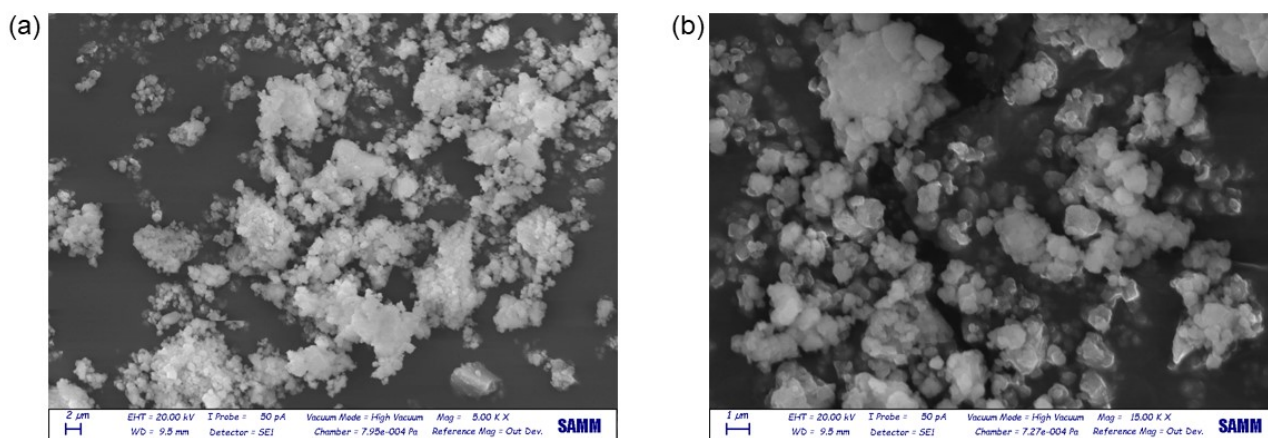


**Figure S1.** SEM of the amorphous phase **a1** obtained upon LAG.

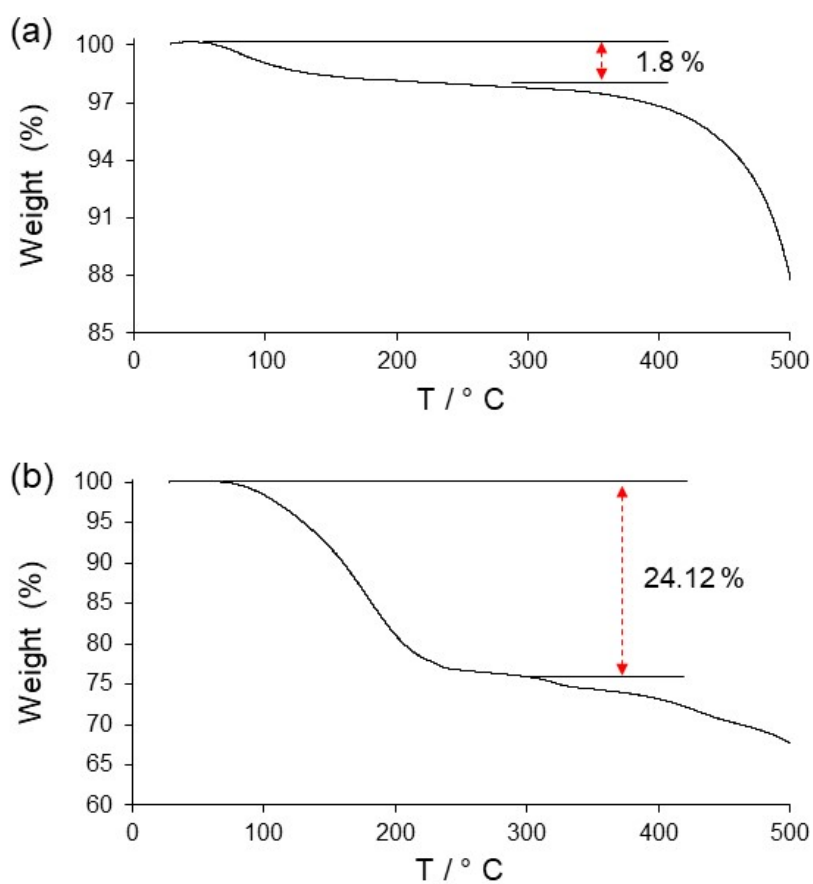


**Figure S2.** TGA data carried out on the amorphous phase **a1** obtained upon LAG (a) and after **a1** is immersed in 1,2-dichlorobenzene (b).

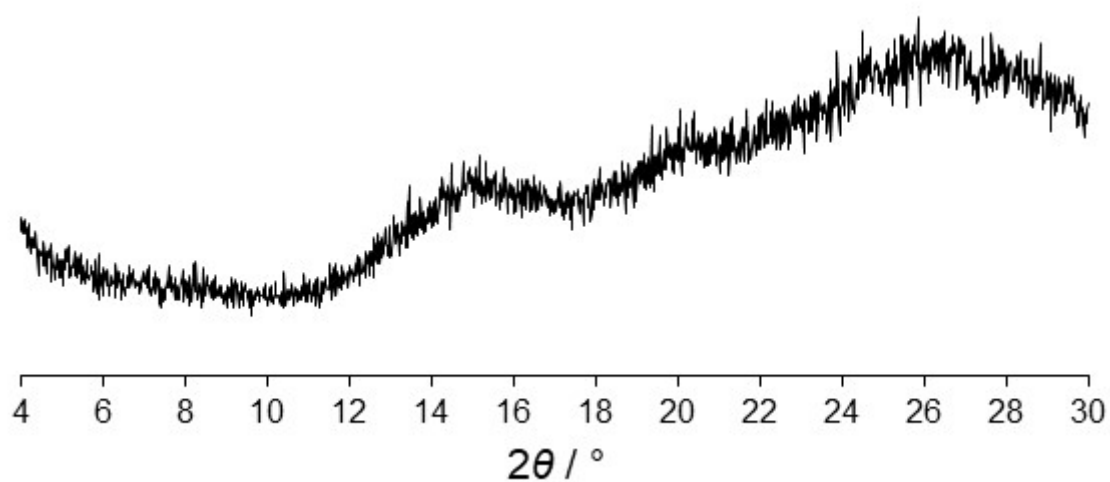


**Figure S3.** Powder XRD plot of the **a1** product obtained using  $5\mu\text{L}$  of 1,2-dichlorobenzene for the LAG reaction.

## Single crystal X-ray structure of **1** including 1,2-dichlorobenzene.

The single crystal X-ray structure of the poly- $[n]$ -catenane containing 1,2-dichlorobenzene depicting only the asymmetric unit is shown in Figure S4. **1** is isostructural to the previously reported TPB-ZnCl<sub>2</sub> poly- $[n]$ -catenane.<sup>1</sup>

The unit cell was indexed successfully with the following parameters (100 K):  $a = 37.9184(11)$  Å,  $b = 37.9184(11)$  Å,  $c = 16.6172(9)$  Å,  $\alpha = 90^\circ$ ,  $\beta = 90^\circ$ ,  $\gamma = 120^\circ$ ,  $V = 20691$  Å<sup>3</sup> with space group  $R-3$ . In the asymmetric unit there are 1.3 **TPB**, two ZnBr<sub>2</sub> and two 1,2-dichlorobenzene molecules crystallographically independent with occupancies 0.86 and 0.4. Electron density corresponding to a disordered 1,2-dichlorobenzene with low occupancy amounting to a total of C2.13, H1.39, Cl0.57 per 1,2-dichlorobenzene. CCDC: 2107305

## Mechanochemical synthesis of amorphous poly- $[n]$ -catenane (**a1**) using neat grinding.

The neat grinding reaction has been carried out grinding **TPB** (30 mg) and ZnBr<sub>2</sub> (33 mg) for (15 mins) and the product (**a1**) checked by powder XRD. The comparison of **a1** against the experimental powder XRD data of **TPB** shows the amorphous nature of the product (Figure S4).

The white raw product has been weighted right after the neat grinding with 62 mg obtained. Because below 10 % of crystalline **TPB** material cannot be detected by powder XRD, to remove any unreacted **TPB** or ZnBr<sub>2</sub> the solid product was immersed and stirred in a mixture chloroform (5 ml) and methanol (1 ml) overnight. Then the product was left to equilibrate with atmosphere overnight and carried out powder XRD experiments which showed that the material was amorphous with a diffraction pattern very similar to the original phase (Figure S4). The collected sample is 51 mg. Yield based on **TPB**: 81.3 %. The elemental analysis results confirms that the amorphous phase after

purification corresponds to the chemical formula  $(\text{TPB})_2(\text{ZnBr}_2)_3$ . Calcd: C 38.98, N 6.49, H 2.34; found: C 38.90, N 6.23, H 1.99.

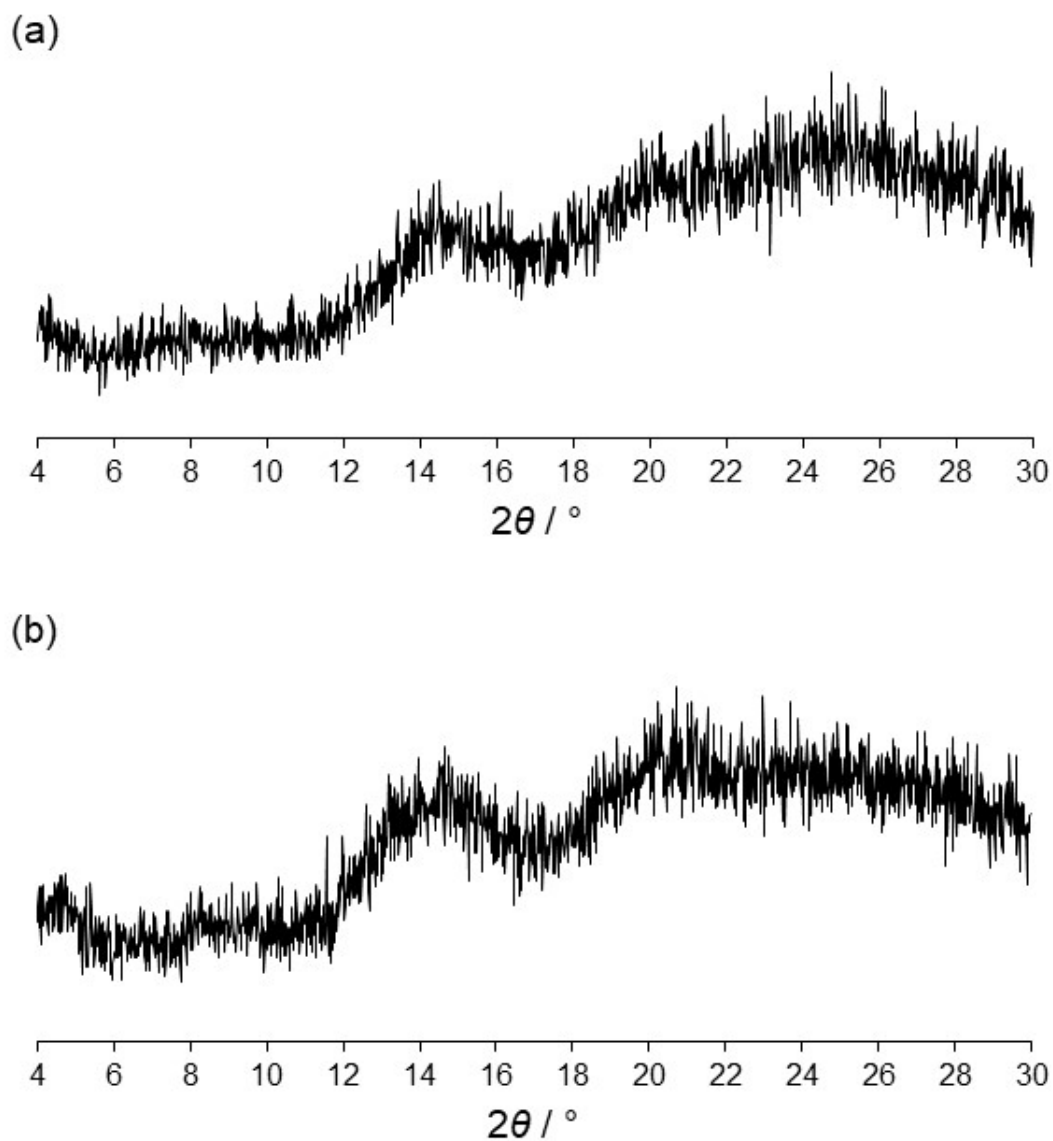


**Figure S4.** (a) Powder XRD pattern of the as synthesized amorphous phase **a1** by neat grinding and (b) powder XRD pattern of **a1** washed in a suspension of chloroform/methanol. First experiment named NG1 in Table S1.

The neat grinding was repeated for another two experiments following the same procedure giving similar yields (Figures S5 and S6). A LAG experiment shows similar results after purification in chloroform/methanol. Table S1 gives an overview of all the neat grinding experiments.

**Table S1.** Summary of the neat grinding experiments carried out in this work.

<b>Sample</b>	<b>TPB</b>	<b>ZnBr<sub>2</sub></b>	<b>Raw Product</b>	<b>Washed Product*</b>	<b>Yield</b>
<b>NG1</b>	30 mg	33 mg	62 mg	51 mg	81.3 %
<b>NG2</b>	30 mg	33 mg	63 mg	50 mg	79.7 %
<b>NG3</b>	30 mg	34 mg	64 mg	52 mg	82.9%

\* We note that our estimation of product that cannot be recovered (*i.e.*, product attached to the round bottom flask and lost in the filter paper) after washing the raw product is *ca.* 2-3 mg, which means that the yield is slightly higher.

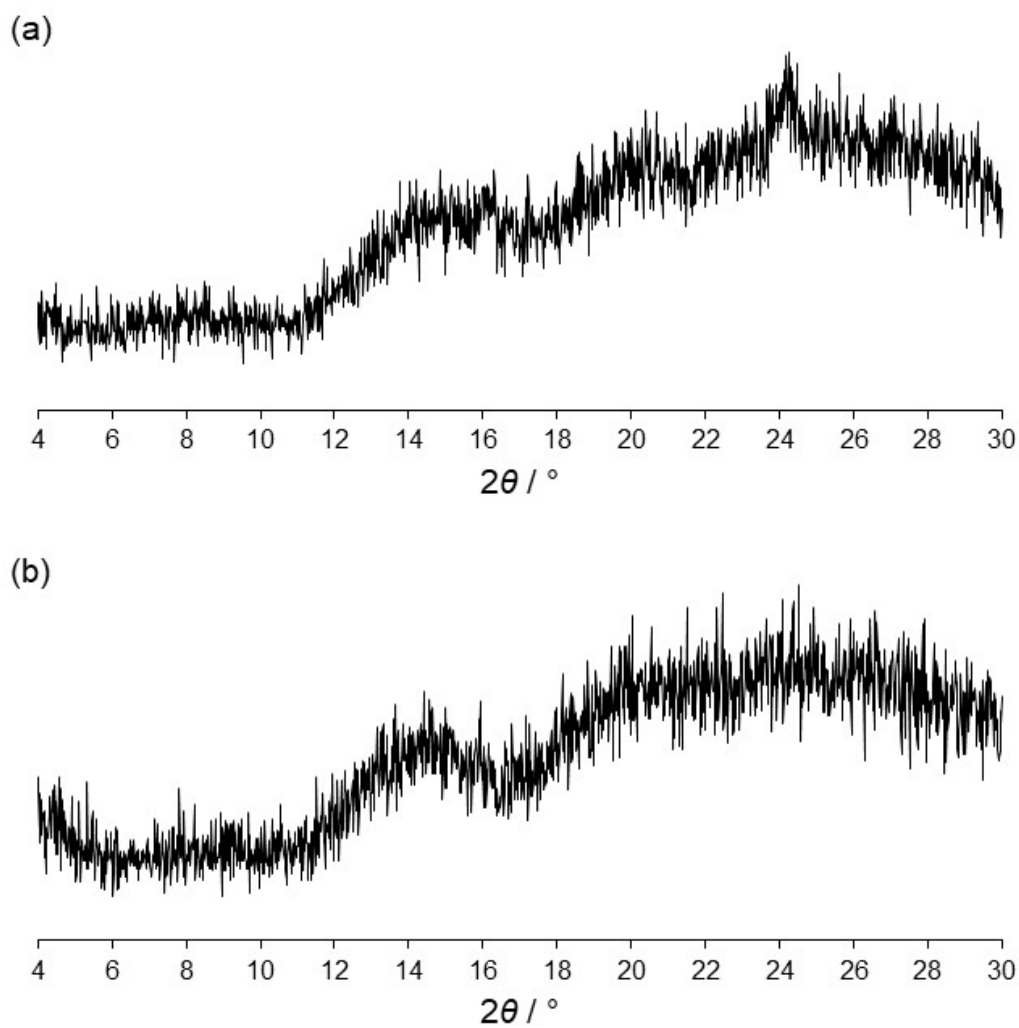


**Figure S5.** (a) Powder XRD pattern of the as synthesized amorphous phase **a1** by neat grinding and (b) powder XRD pattern of **a1** washed in a suspension of chloroform/methanol. Second experiment named NG2 in Table S1.

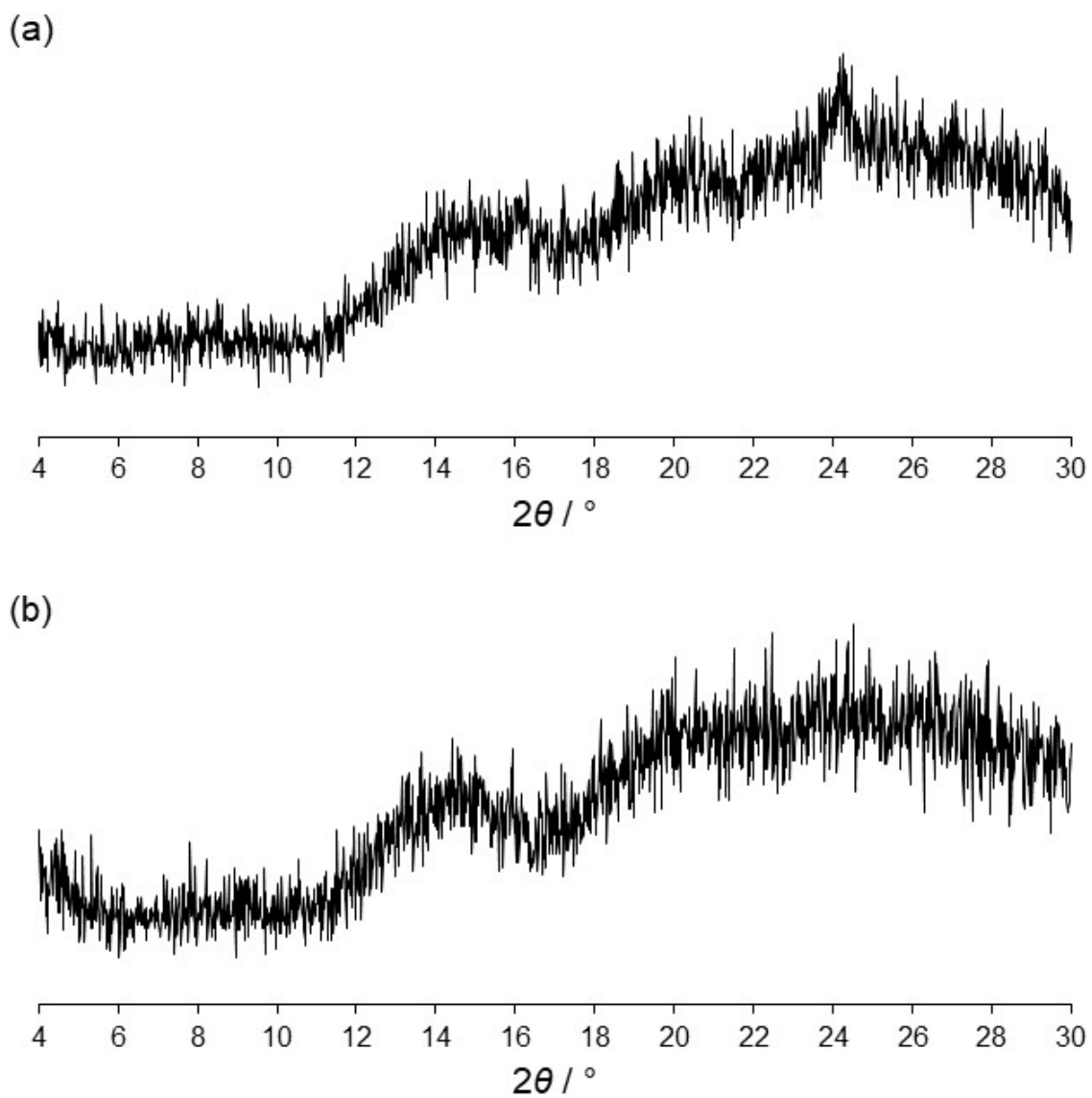


**Figure S6.** (a) Powder XRD pattern of the as synthesized amorphous phase **a1** by neat grinding and (b) powder XRD pattern of **a1** washed in a suspension of chloroform/methanol. Third experiment named NG3 in Table S1.

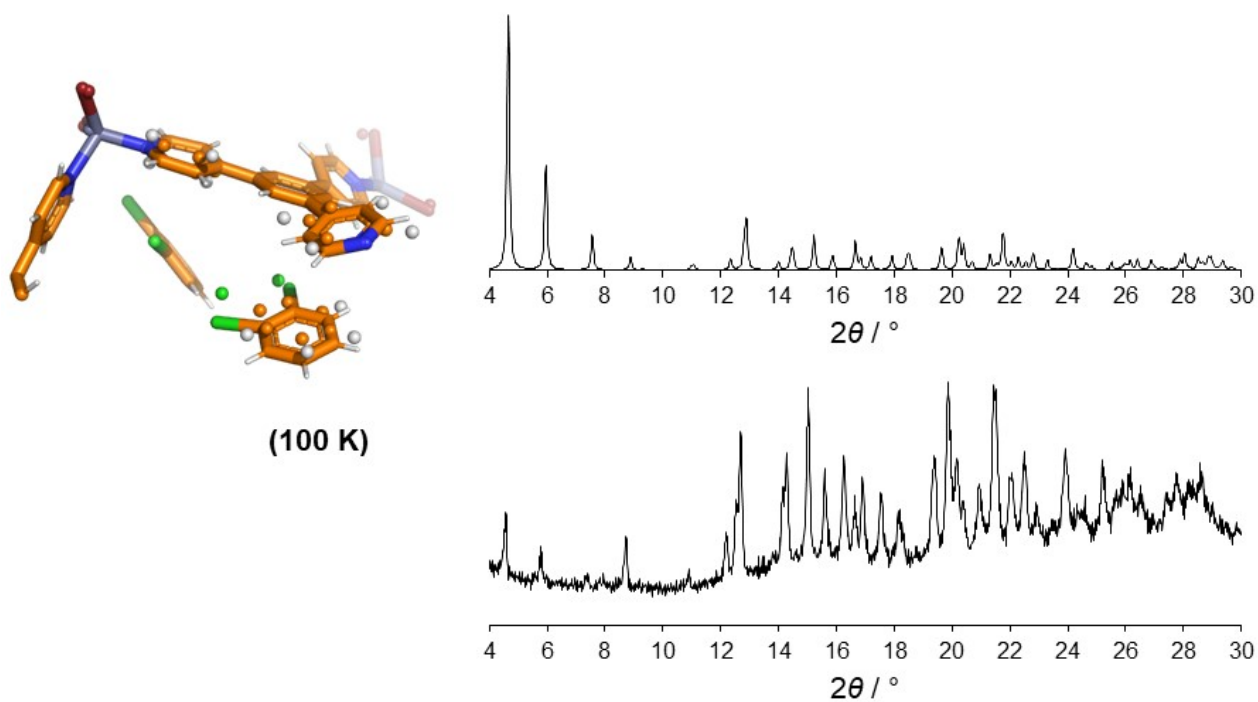


**Figure S7.** Simulated powder XRD of a single crystal containing 1,2-dichlorobenzene (**1**) compared against the experimental powder data obtained from the amorphous to crystalline transformation from **a1** to **1**.

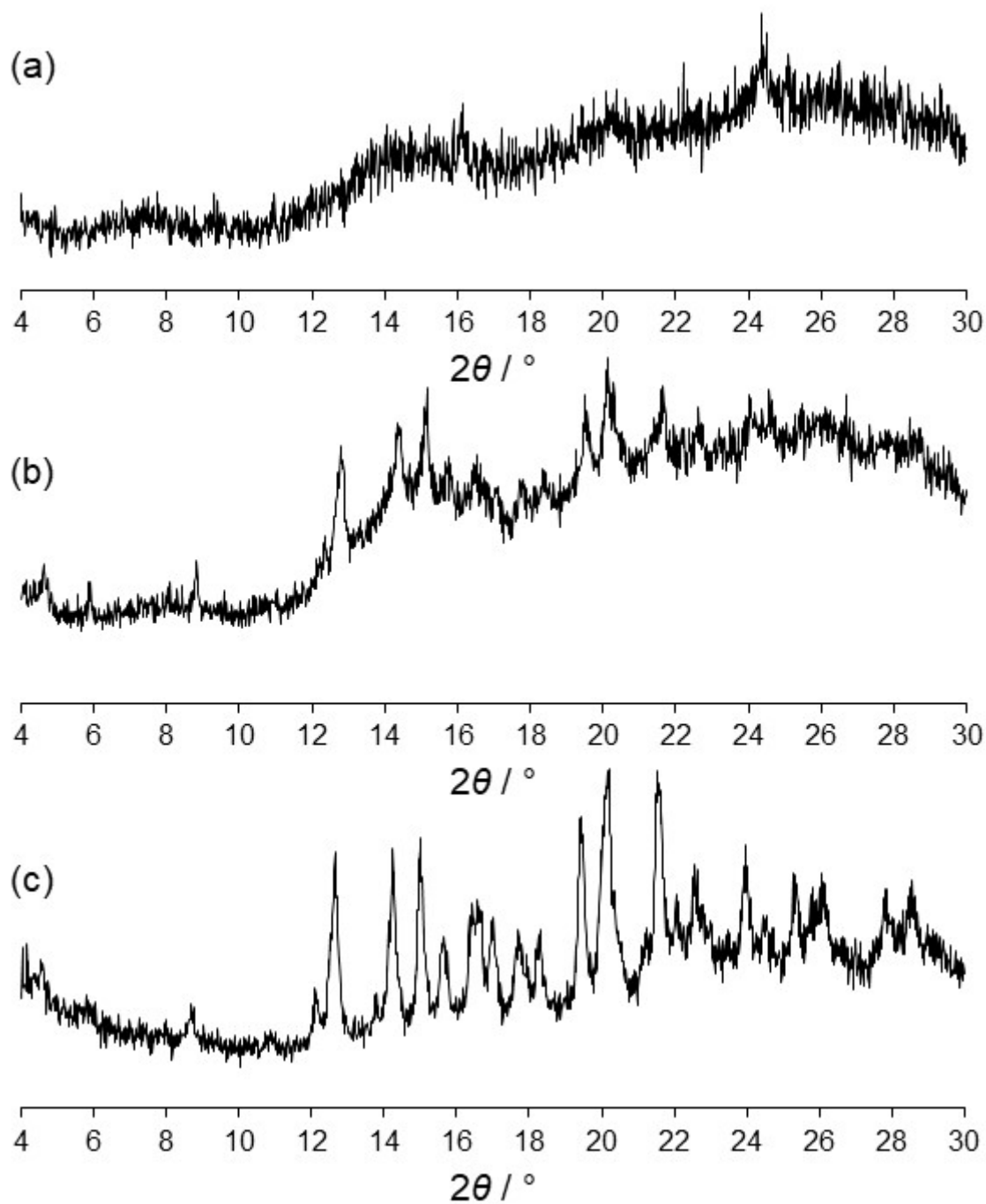


**Figure S8.** Powder XRD plot showing the reconstruction of the amorphous phase (**a1**) obtained by neat grinding (a). Diffractogram obtained after **a1** was immersed in 1,2-dichlorobenzene for 2 days (b). The powder XRD pattern of the sample shown in (b) after immersing it in a mixture 1,2-dichlorobenzene/methanol (3ml:3ml) (c). The weak peak in (a) at  $2\theta = 24.45^\circ$  corresponds to small quantity of unreacted **TPB**.

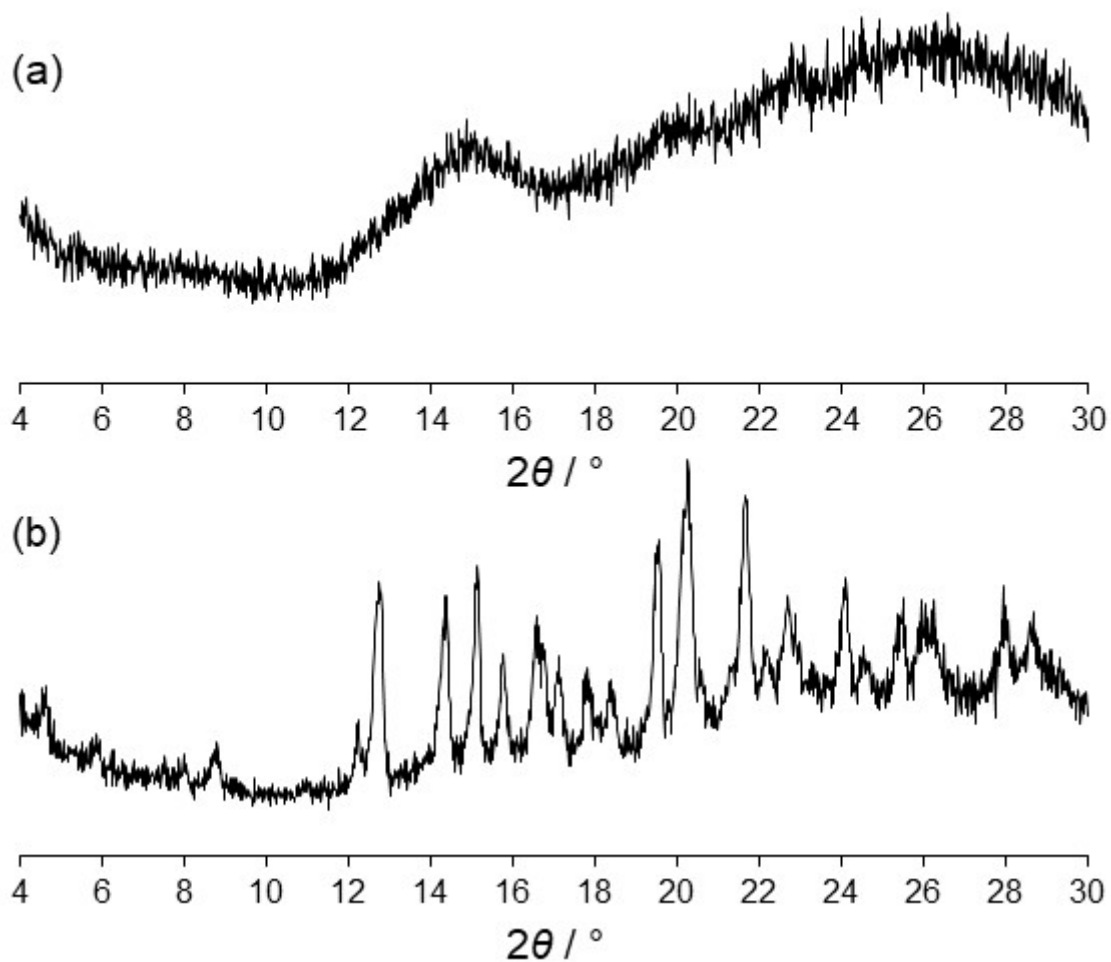


**Figure S9.** Powder XRD plot of the **a1** product obtained using  $5\mu\text{L}$  of 1,2-dichlorobenzene for the LAG reaction immersed in 1,2-dichlorobenzene for 4 days (a). The same sample immersed in a mixture 1,2-dichlorobenzene/methanol (3ml:3ml) for one day (b).

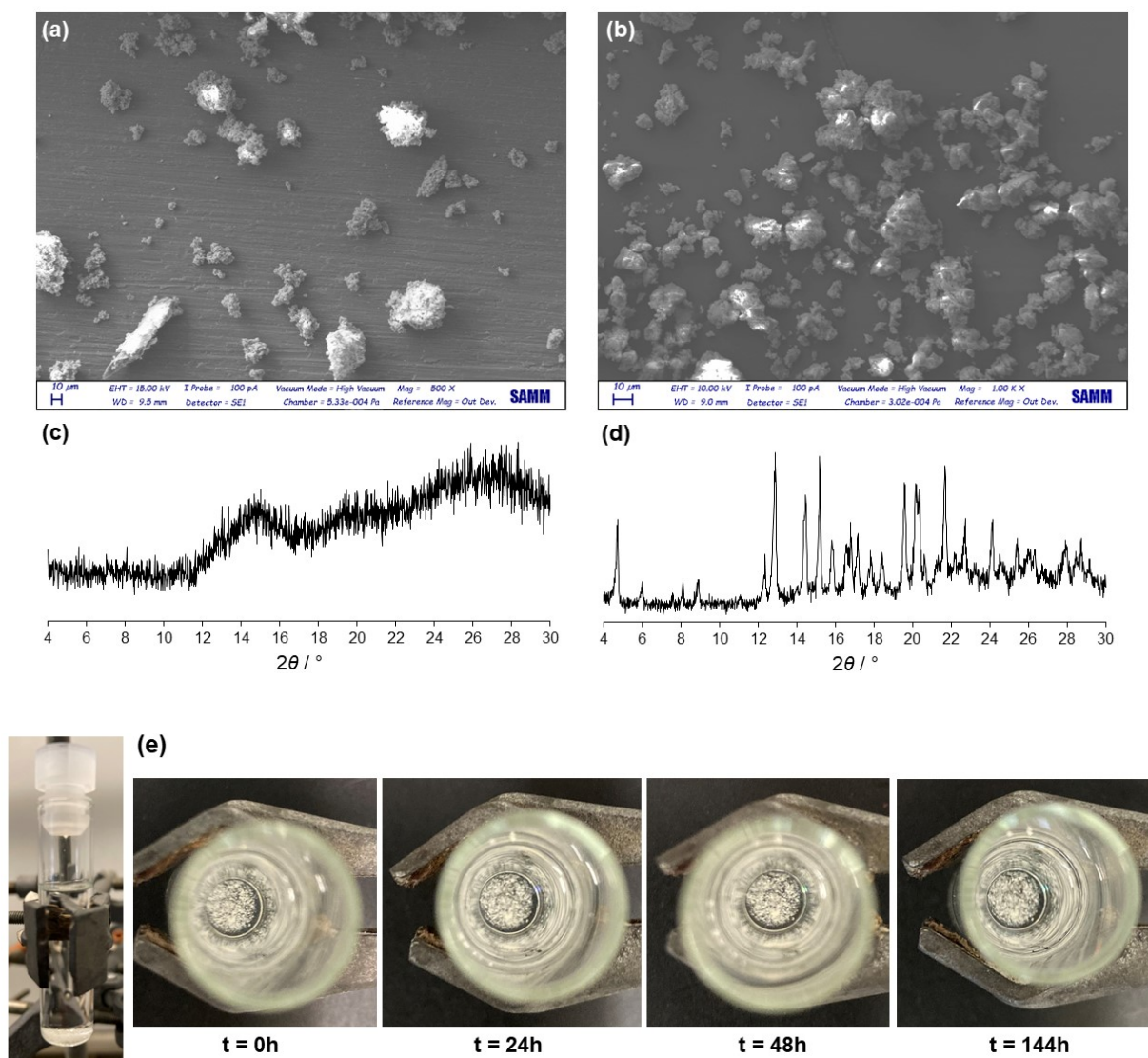


**Figure S10.** SEM images of an amorphous phase (a1) obtained by neat grinding (a) and the same sample after undergoing the *amorphous-to-crystalline* transformation by uptaking 1,2-dichlorobenzene (b). The image shows how the habit of the particles did not change due to recrystallization process. Plots showing the powder XRD of the amorphous phase (c) and after the uptake of 1,2-dichlorobenzene (d). Pictures taken after 24 h interval time in which 2 mg of amorphous phase are immersed in a 2:2 ml of 1,2-dichlorobenzene/methanol solution (e). After six days no change is observed in the suspension indicating that no dissolution or crystallization of the amorphous phase takes place.

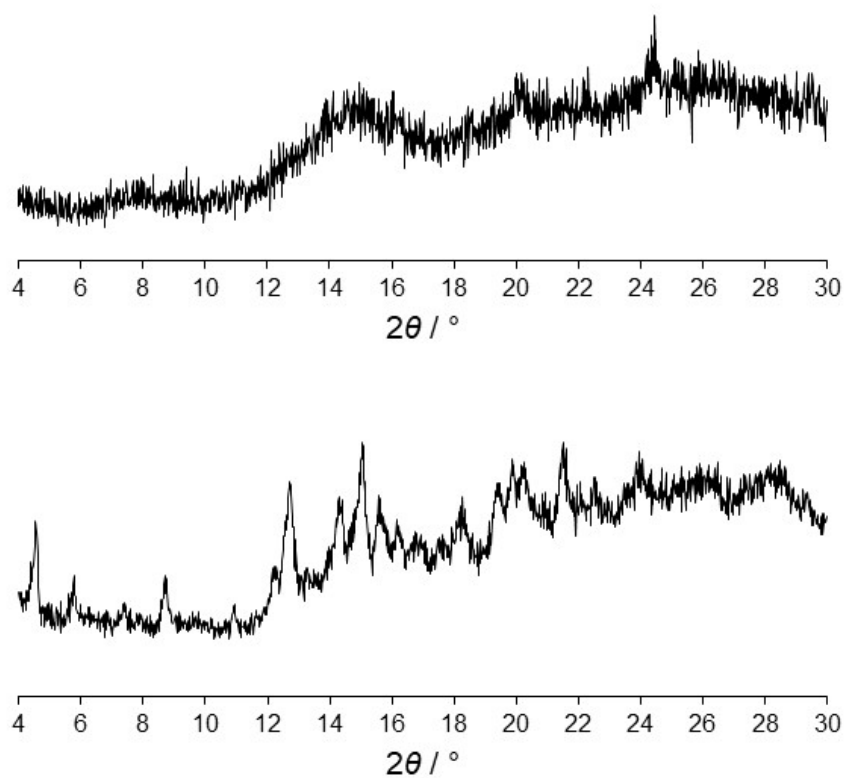


**Figure S11.** Powder XRD of **a1** prepared by neat grinding and the diffractogram obtained upon gas-solid reaction by exposing **a1** to a mixture of methanol:1,2-dichlorobenzene. The weak peak in (a) at  $2\theta = 24.45^\circ$  corresponds to small quantity of unreacted **TPB**.

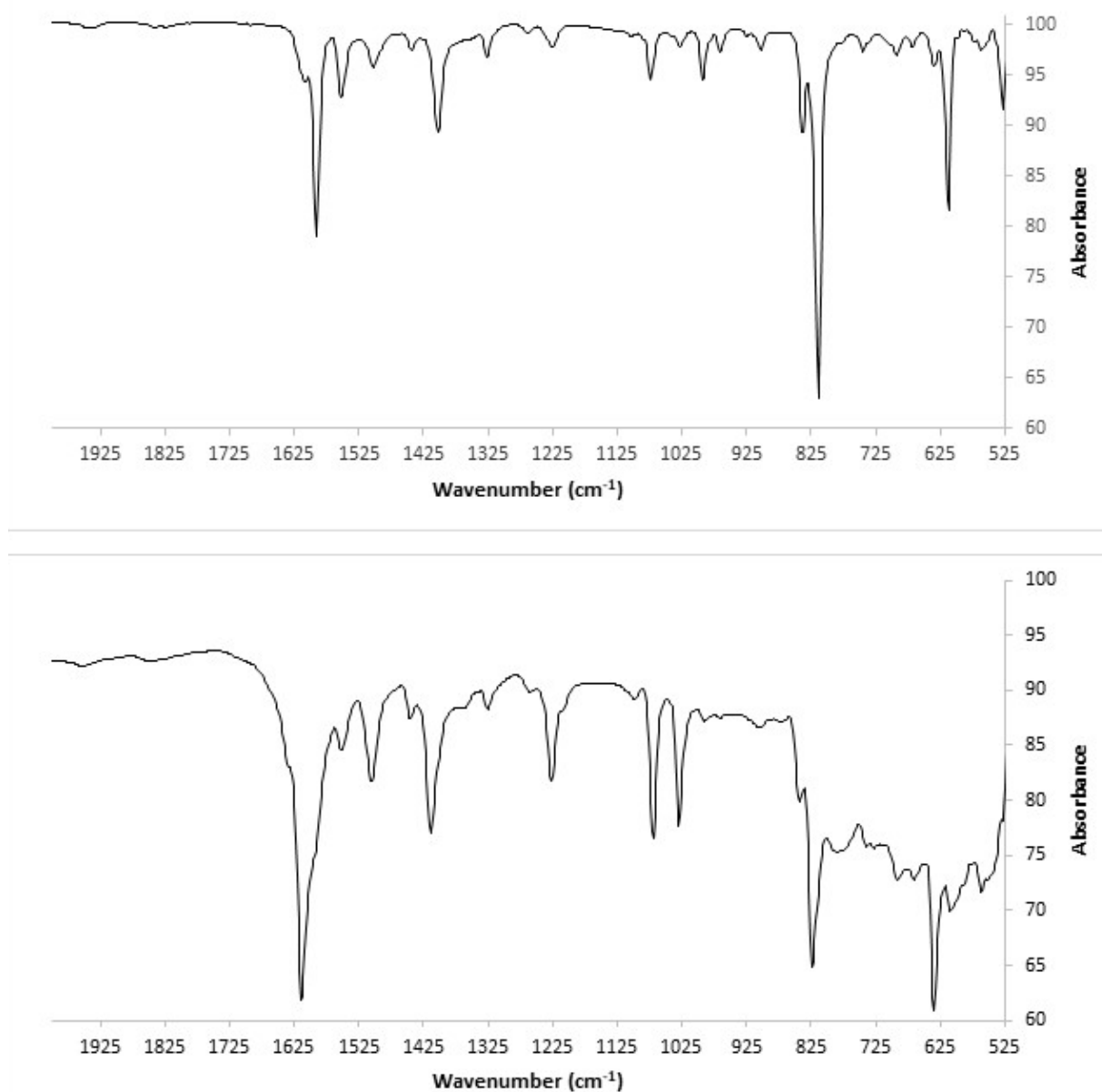


**Figure S12.** ATR-FT-IR corresponding to ligand **TPB** (top) vs amorphous **a1** (bottom).

### **ATR-FT-IR data of TPB, 1 and a1.**

IR experiments have been carried out for the **TPB** ligand, the crystalline poly- $[n]$ -catenane and for the amorphous phase. The FT-IR spectrum of the free ligand showed two strong bands at  $1591\text{ cm}^{-1}$  (with a shoulder at  $1608\text{ cm}^{-1}$ ) and  $814\text{ cm}^{-1}$  which can be ascribed to skeletal vibrations of the aromatic rings and to the aromatic CH scissoring respectively. For the crystalline poly- $[n]$ -catenane sample, these two bands were slightly shifted to  $1612\text{ cm}^{-1}$  and  $825\text{ cm}^{-1}$ . Besides, two new intense signals at  $750\text{ cm}^{-1}$  and  $634\text{ cm}^{-1}$  appeared.

In particular, this last band has been assigned in the literature to the formation of pyridine-metal complex<sup>2</sup>.

Comparison of the spectrum of the crystalline phase with the amorphous one, revealed some similarities, in particular the presence of the bands at 1614, 1030, 815 and 634  $\text{cm}^{-1}$ . The weak band at 1124  $\text{cm}^{-1}$  and the strong band at 750  $\text{cm}^{-1}$  is from 1,2-dichlorobenzene which is not observed in the amorphous phase as it is synthesized without solvent. Thus, the good match in the IR both crystalline and amorphous phases is supporting the formation of a similar metal-ligand complex in both samples. So we can confirm the formation of the catenane in the amorphous phase.

**TPB:** IR – ATR: 1608 w, 1591 s, 1552 w, 1444 w, 1402 m, 1327 w, 1225 w, 1074 w, 993 w, 838 w, 813 s, 611 m, 528 w.

**Crystalline:** IR – ATR: 1612 s, 1552 w, 1504 w, 1454 w, 1414 m, 1323 w, 1223 m, 1124 w, 1068 m, 1028 m, 825 s, 750 s, 634 s.

**Amorphous:** IR – ATR: 1614 s, 1551 w, 1504 w, 1444 w, 1413 m, 1327 w, 1221 w, 1068 m, 1028 m, 823 s, 634 m.

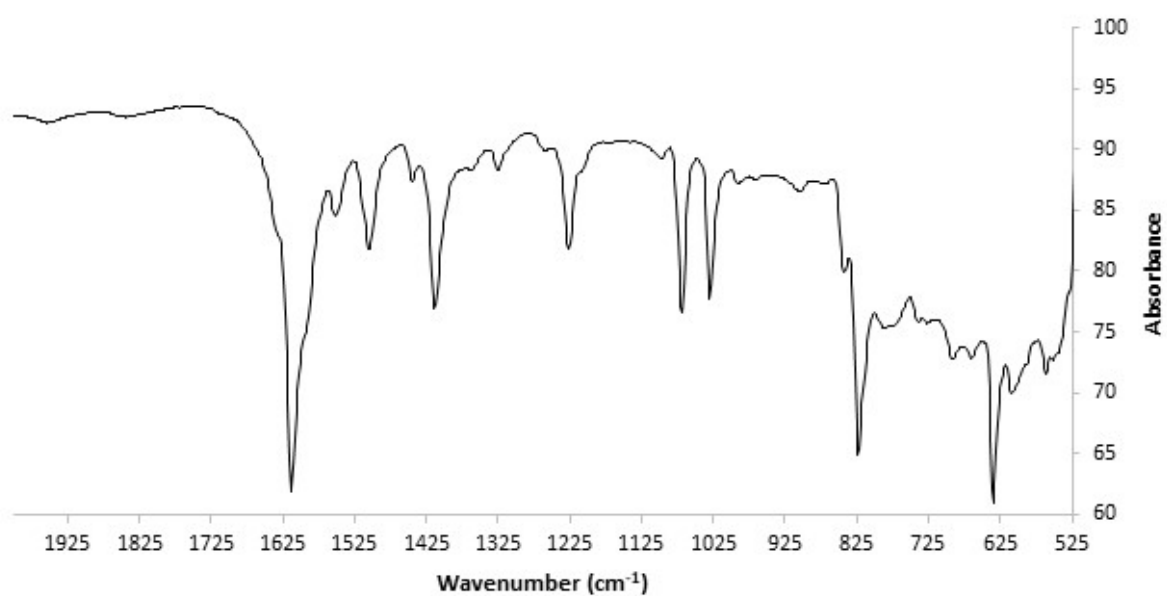
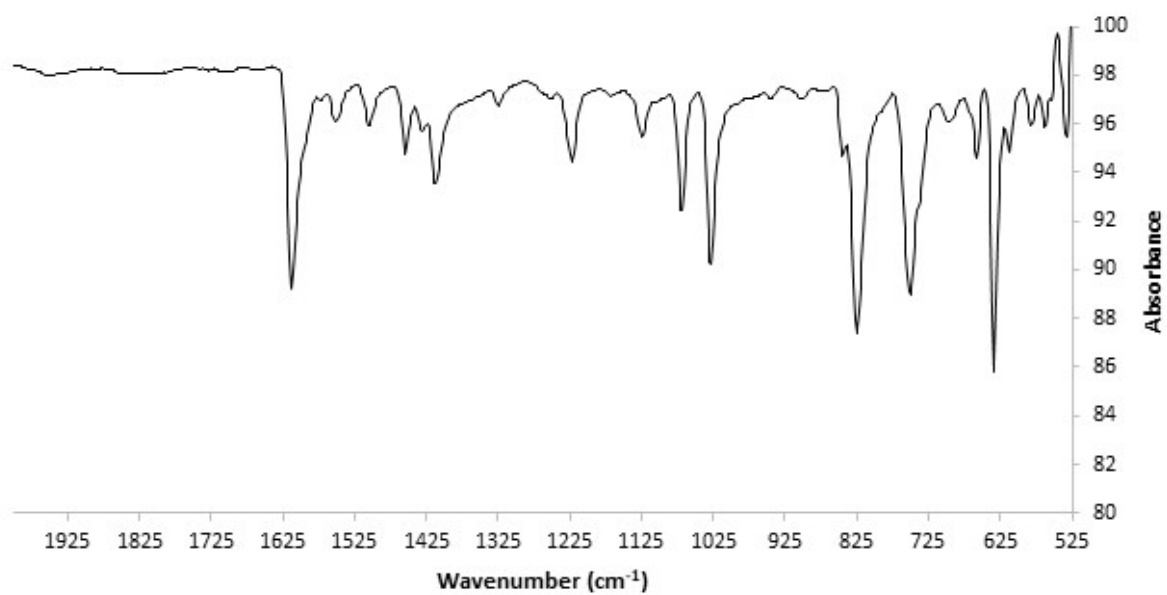


**Figure S13.** ATR-FT-IR corresponding to ligand crystalline **1** (top) vs amorphous **a1** (bottom).

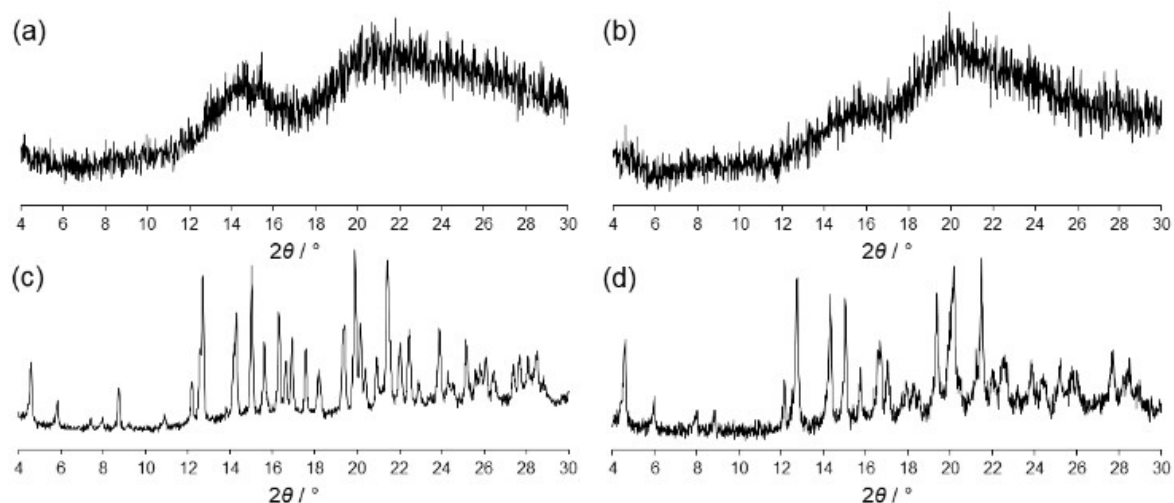


**Figure S14.** Powder XRD patterns of the amorphous poly-[*n*]-catenane **1** obtained using chloroform/methanol (a) and chloroform/18-crown-6 (b) and their crystalline transformation giving the poly-[*n*]-catenane when immersed in *p*-chlorotoluene (c) and 1,2-dichlorobenzene (d).

### **Instant synthesis of poly-[*n*]-catenane including 1,2-dichlorobenzene as templating molecule.**

Thus, the ability to crystallize isostructural **MIMs** as powders has been tested in poly-[*n*]-catenanes assembled of **TPB** and  $\text{ZnBr}_2$ . Ligand **TPB** (0.097 mmol) is dissolved in a mixture of 1,2-dichlorobenzene and methanol (8:2 mL), and then a methanolic solution of  $\text{ZnBr}_2$  (0.1455 mmol in 2 mL of MeOH) was added instantaneously into the vigorously stirring solution of **TPB**. After filtration 61.16 mg of crystalline product was collected (Figure S15).

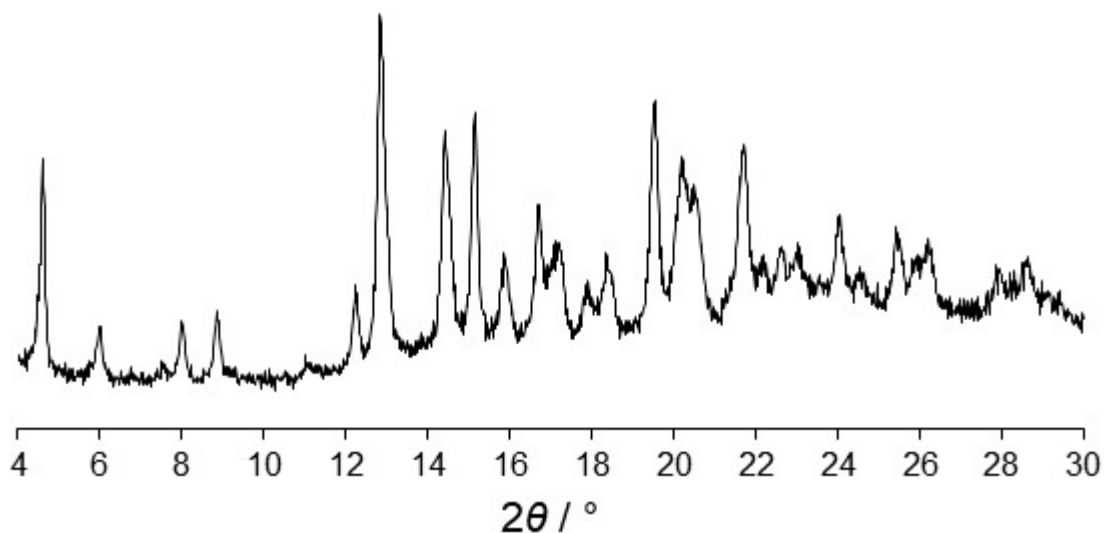


**Figure S15.** Powder XRD pattern of **1** synthesized using the instant synthesis method using 1,2-dichlorobenzene as templating molecule.

The TG plot shows that there are two main different slopes in the weight release (30.2 %; *ca.* 2 guests) of 1,2-dichlorobenzene which clearly indicates that in the cages there are two different guests from a crystallographic point of view (Figure S16a).

Using the unit cell of **1** (100 K), a LeBail refinement was carried out to check the purity of the microcrystalline product obtained from the instant synthesis at 300 K. Crucially, as seen in the refinement plot (Figure 16b), the LeBail refinement shows a good fitting against the experimental data ( $R_{wp} = 6.37\%$ ), indicating that there is no presence of other crystalline phases in the bulk material.

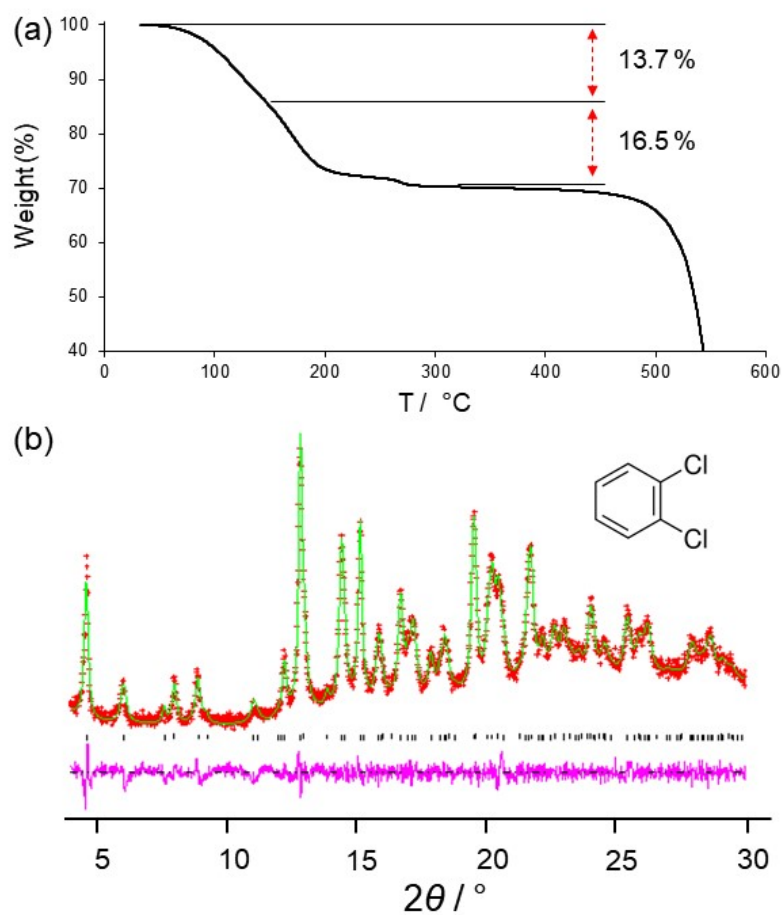


**Figure S16.** (a) TG plot showing the two slopes of guest release and (b) LeBail refinement of the product obtained from the instant synthesis method using 1,2-dichlorobenzene as templating solvent.

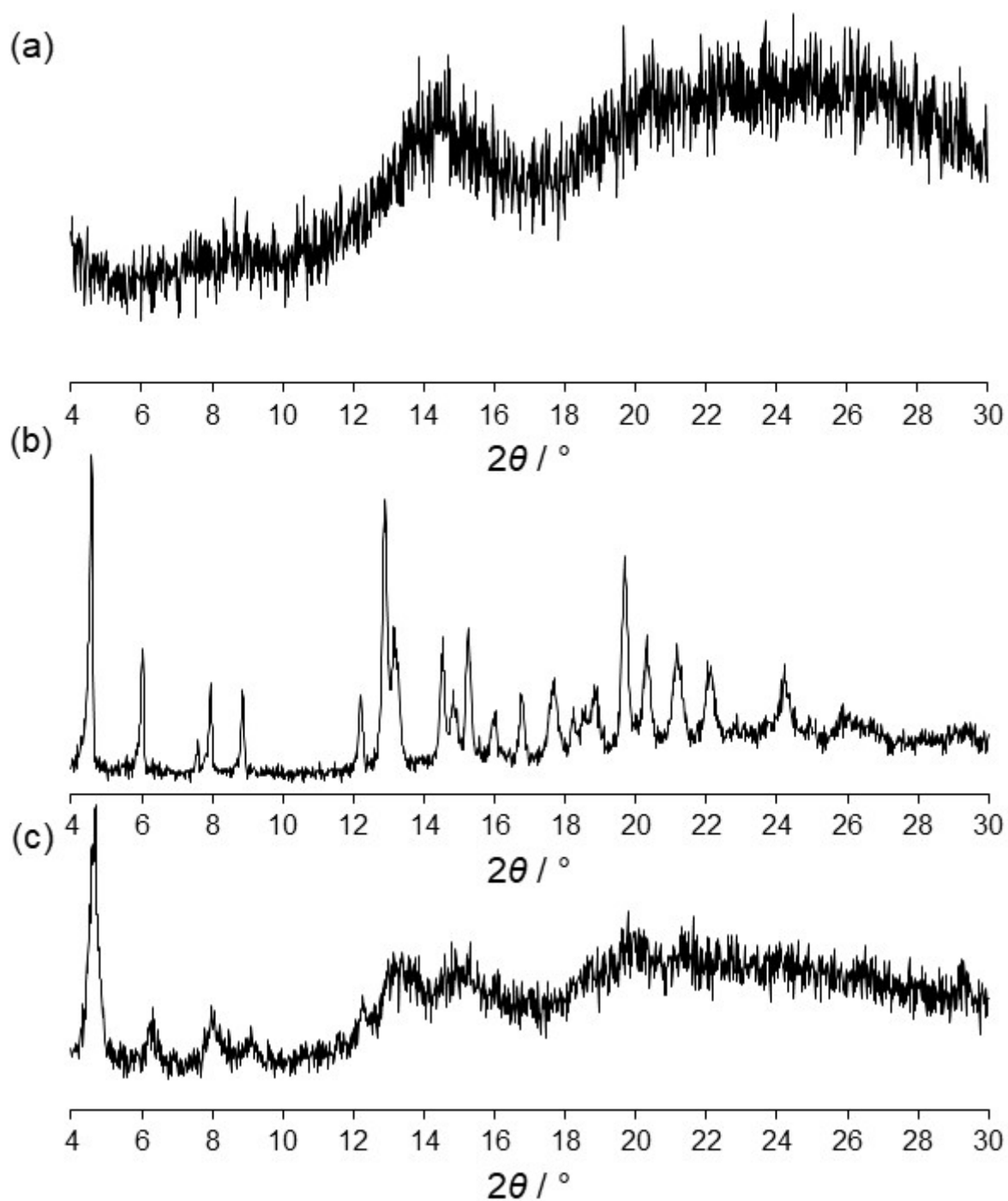


**Figure S17.** Powder XRD plot showing how the poly-[*n*]-catenane can be reconstructed if **a1** is immersed in methanol overnight. Amorphous phase obtained upon neat grinding (a), crystalline phase after immersing the amorphous phase in methanol (b) and the partially crystalline phase after *ca.* 30 minutes in contact with air at r.t. (c).

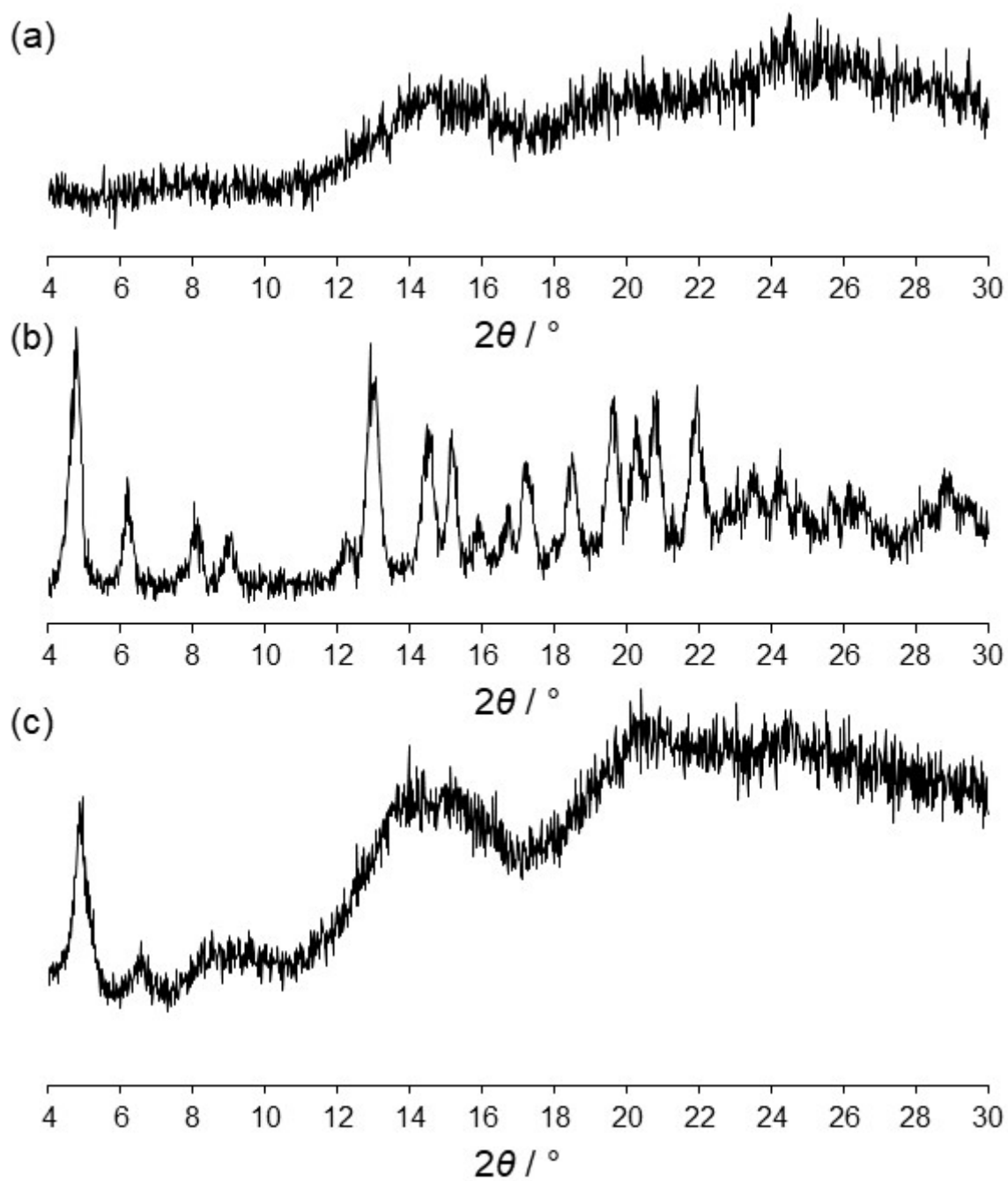


**Figure S18.** Powder XRD plot showing how the poly-[*n*]-catenane can be reconstructed if **a1** is immersed in ethanol overnight. Amorphous phase obtained upon neat grinding (a), crystalline phase after immersing the amorphous phase in ethanol (b) and the partially crystalline phase after *ca.* 30 minutes in contact with air at r.t. (c).

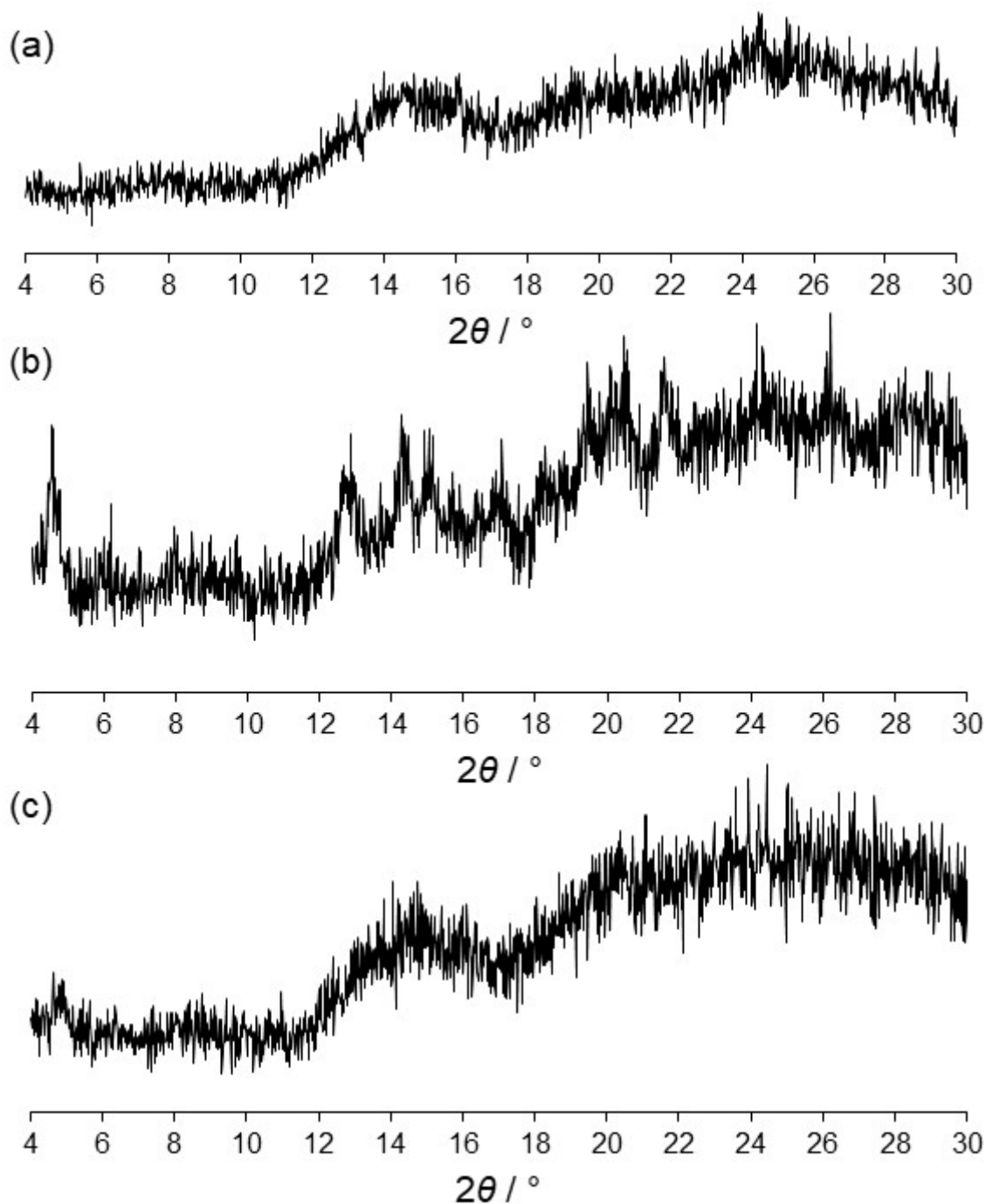


**Figure S19.** Powder XRD plot showing how the poly-[*n*]-catenane can be reconstructed if **a1** is immersed in isopropanol overnight. Amorphous phase obtained upon neat grinding (same batch of Figure S18) (a), crystalline phase after immersing the amorphous phase in isopropanol (b) and the amorphous phase after *ca.* 30 minutes in contact with air at r.t. (c).

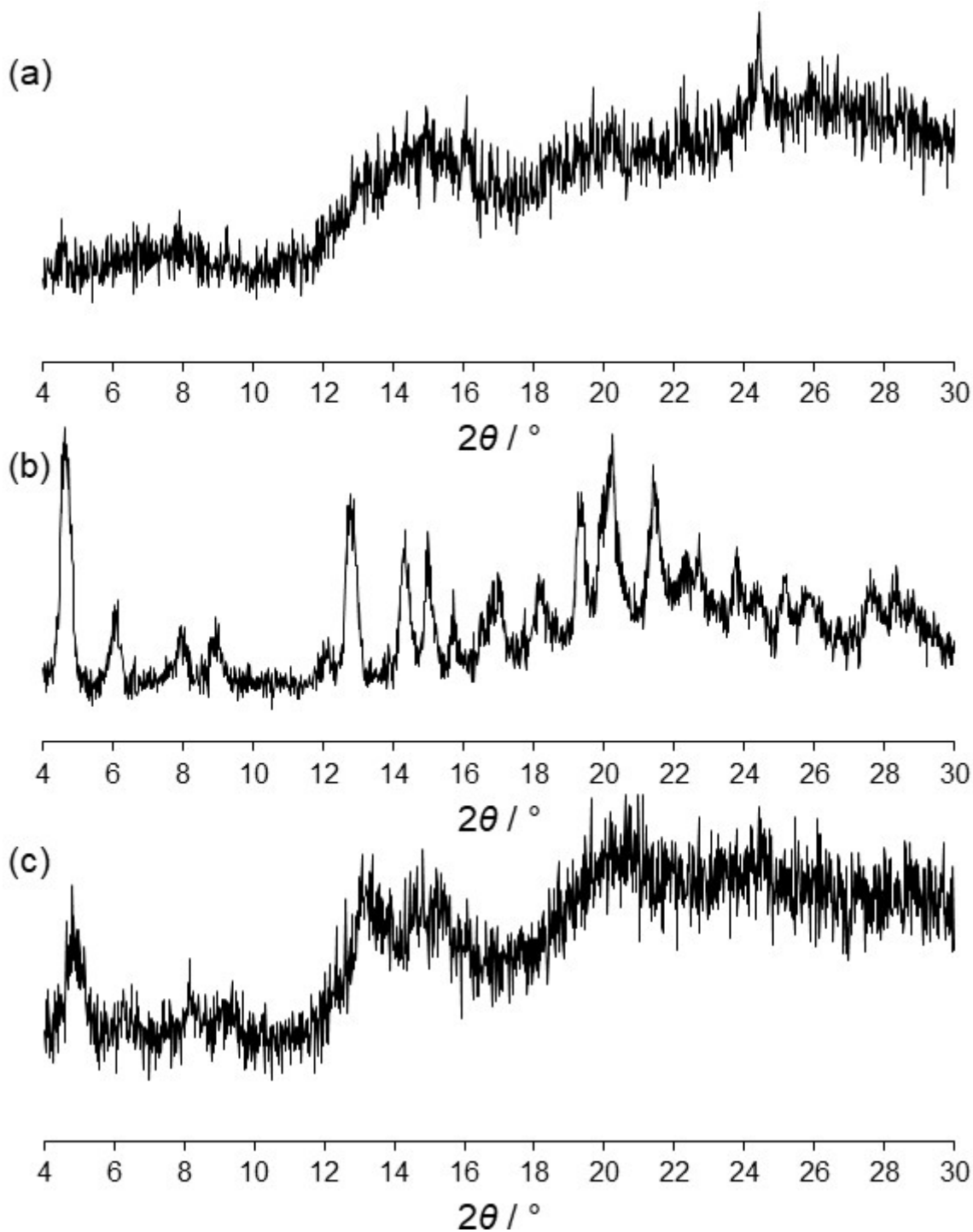


**Figure S20.** Powder XRD plot showing how the poly-[*n*]-catenane which is reconstructed if **a1** is immersed in propanol overnight. Amorphous phase obtained upon neat grinding (a), crystalline phase after immersing the amorphous phase in propanol (b) and the amorphous phase after *ca.* 30 minutes in contact with air at r.t. (c). The weak peak in (a) at  $2\theta = 24.45^\circ$  corresponds to small quantity of unreacted **TPB**.

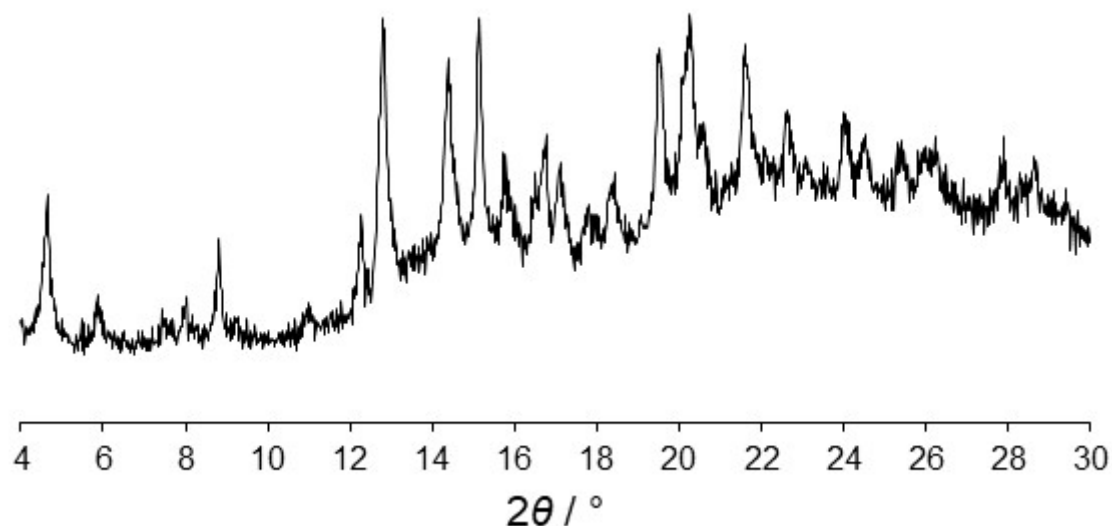


**Figure S21.** Powder XRD plot showing the crystalline phase obtained after immersing the amorphous phase shown in Figure S19c in a mixture isopropanol/1,2-dichlorobenzene (3ml:3ml). The reconstructed poly-[*n*]-catenane is stable at r.t. for several days.

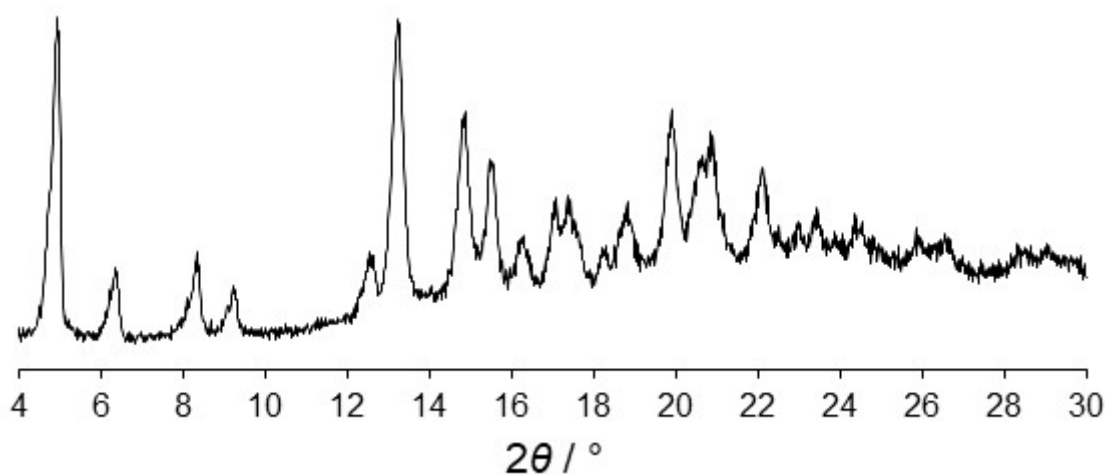


**Figure S22.** Powder XRD plot showing the crystalline phase obtained after immersing the amorphous phase shown in Figure S20c in a mixture methanol/toluene (3ml:3ml). The reconstructed poly-[*n*]-catenane is stable at r.t. for several days.

## High-resolution solid-state NMR

The  $^{13}\text{C}$  CPMAS and CPMAS NQS spectra of **TPB** is shown in Figure S23. High resolution spectra are observed under CP conditions indicating that **TPB** has a crystalline form. The quaternary carbon atoms are assigned using the CPMAS NQS spectrum. The quaternary pyridines carbons are observed at 148.7 ppm, the CH (next to the nitrogen) at 150.4 ppm. The quaternary carbons of the benzene ring are at 143.1, 139.3 and 136.2 ppm while the remaining (pyridine and benzene) CH fall in the range 126.2-119.2 ppm.

The temperature dependence solid state  $^{13}\text{C}$  HPDEC NMR spectra of **1** is shown in Figure S25 which shows that the sharp peaks corresponding to the guest molecules become slightly broader as they become less mobile.

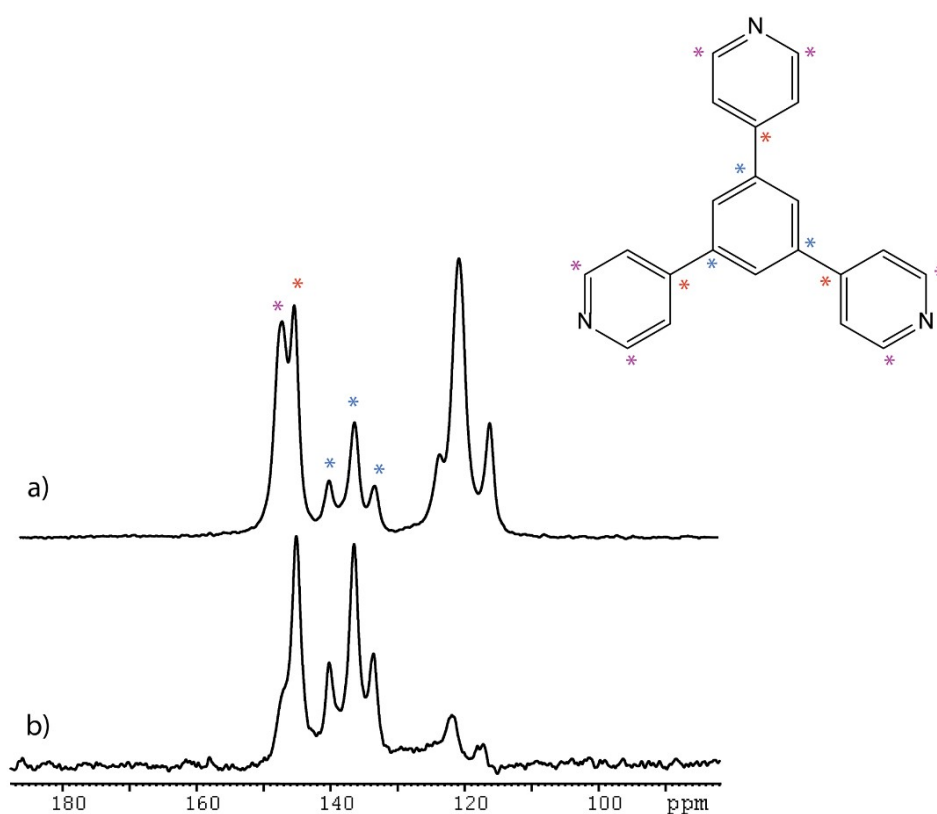


**Figure S23.**  $^{13}\text{C}$  solid state NMR spectra of the ligand **TPB**: a) CPMAS, b) CPMAS NQS spectra.

**TPB** chemical structure and peaks assignment is also shown.

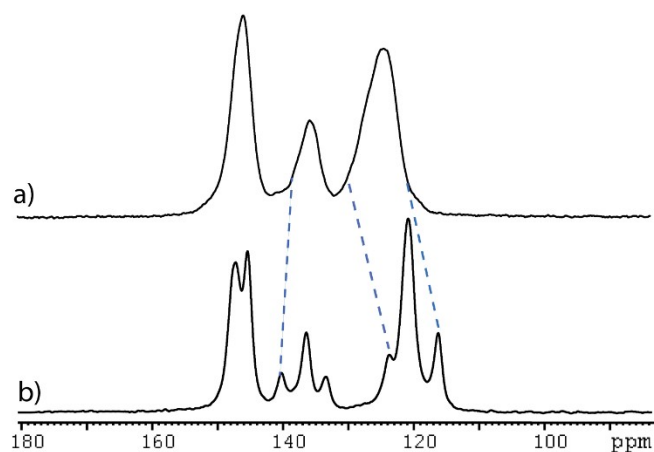


**Figure S24.**  $^{13}\text{C}$  CPMAS spectra of the amorphous poly- $[n]$ -catenane **a1** (a) and **TPB** (b). Chemical shift variation are highlighted.

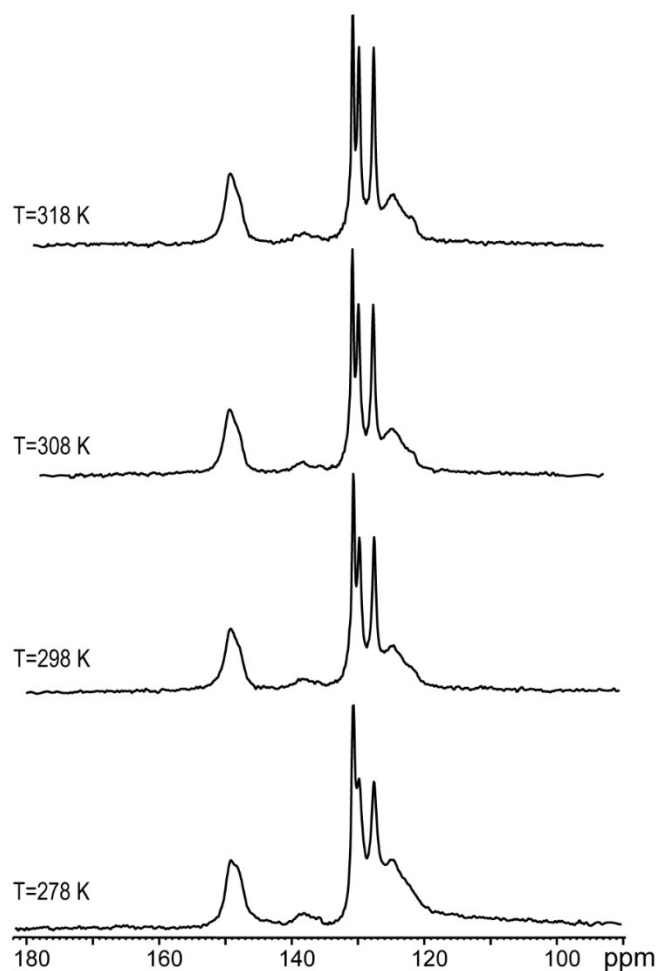


**Figure S25.** Solid state  $^{13}\text{C}$  HPDEC NMR spectra of the crystalline poly- $[n]$ -catenane **1** in the temperature range 278-318 K.

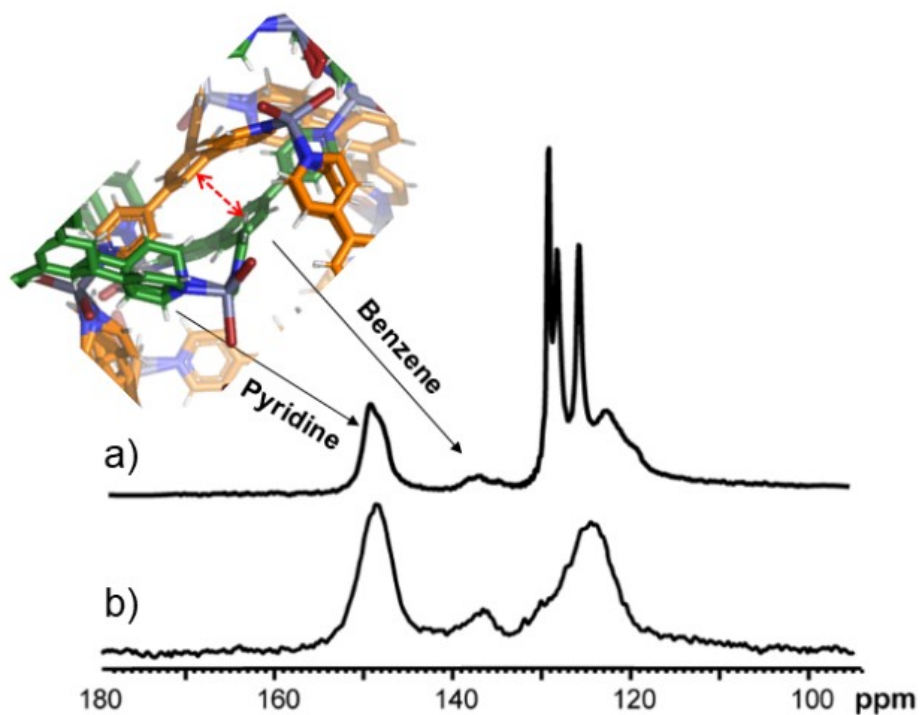


**Figure S26.** Solid state  $^{13}\text{C}$  HPDEC MAS NMR spectra (298 K) of the microcrystalline poly- $[n]$ -catenane **1** (a) and amorphous **a1** obtained by neat grinding (b). The inset highlights the higher mobility of the coordinated pyridines vs the less dynamic nature of the central benzene rings in the TPB in a poly- $[n]$ -catenane. In this case the  $\text{M}_{12}\text{L}_8$  framework in the inset is from **1** (100K).

## References

- 1 S. Torresi, S. Famulari, J. Martí-Rujas, *J. Am. Chem. Soc.*, 2020, **142**, 9537-9543.
- 2 C. W. Frank, L. B. Rogers, *Inorg. Chem.*, 1966, **5**, 615-622.